JCI The Journal of Clinical Investigation

αv Integrins regulate germinal center B cell responses through noncanonical autophagy

Fiona Raso, … , Adam Lacy-Hulbert, Mridu Acharya

J Clin Invest. 2018. https://doi.org/10.1172/JCI99597.

Research Article In-Press Preview Immunology Vaccines

Graphical abstract

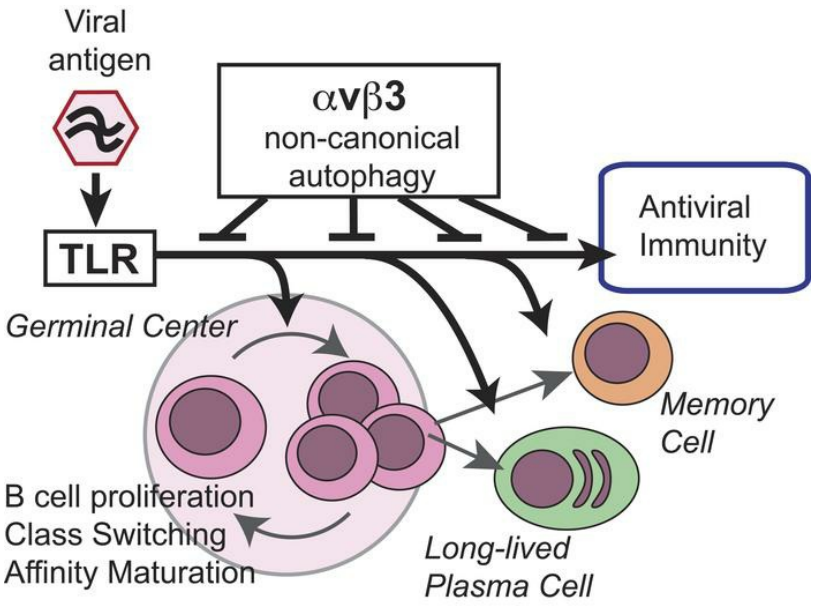

αv integrins regulate germinal center B cell responses through non-canonical autophagy.

Fiona RASO[1], Sara SAGADIEV[1], Samuel DU[2], Emily GAGE [3,4], Tanvi ARKATKAR[2], Genita METZLER[2], Lynda M. STUART[1,5,†], Mark T. ORR[3,4], David RAWLINGS[2,6], Shaun JACKSON[2], Adam LACY-HULBERT[1,6] and Mridu ACHARYA[1†]

1. Immunology Program, Benaroya Research Institute at Virginia Mason, Seattle, WA, USA
2. Seattle Children's Research Institute, Seattle, WA, USA
3. Infectious Disease Research Institute, Seattle, WA, USA
4. Department of Global Health, University of Washington, Seattle, WA, USA
5. Bill and Melinda Gates Foundation, Seattle, WA, USA
6. Department of Immunology, University of Washington, Seattle, WA, USA

[†]Address correspondence to:

Dr Lynda Stuart, Bill and Melinda Gates Foundation, 500 Fifth Ave, Seattle, WA 98109

Telephone: (206) 245 9468

Lynda.stuart@gatesfoundation.org

and

Dr Mridu Acharya, Benaroya Research Institute at Virginia Mason, 1201 Ninth Avenue, Seattle WA 98101

Telephone: (206) 341-8997

macharya@benaroyaresearch.org

Conflict of Interest: Mridu Acharya and Adam Lacy-Hulbert are named as inventors on a provisional patent (No. 62/591620) related to this work filed by Benaroya Research Institute.

Running Title: αv integrins and GC B cell response

Abstract

Germinal centers (GCs) are major sites of clonal B cell expansion and generation of long-lived, high-affinity antibody responses to pathogens. Signaling through toll-like receptors(TLRs) on B cells promotes many aspects of GC B cell responses, including affinity-maturation, class-switching and differentiation into long-lived memory and plasma cells. A major challenge for effective vaccination is identifying strategies to specifically promote GC B cell responses. Here we have identified a mechanism of regulation of GC B cell TLR signaling, mediated by αv integrins and non-canonical autophagy. Using B cell-specific αv-knockout mice, we show that loss of αv-mediated TLR regulation increased GC B cell expansion, somatic-hypermutation, class-switching, and generation of long-lived plasma cells after immunization with virus-like particles(VLPs) or antigens associated with TLR ligand adjuvants. Furthermore, targeting αv-mediated regulation increased the magnitude and breadth of antibody responses to influenza virus vaccination. These data therefore identify a mechanism of regulation of GC B cells, which can be targeted to enhance antibody responses to vaccination.

Introduction

Strong B cell responses are a central component of effective long-lasting immunity to pathogens. B cells possess the unique ability to adapt the sequence of their immune receptors during the course of infection, allowing production of antibodies of increasing affinity to specific epitopes, and greater breadth of binding to similar antigens. In addition, the generation of long-lived plasma and memory B cells allows rapid production of antibodies after subsequent encounters with the same or related pathogens. The generation of these durable, high-affinity antibody responses occurs predominantly in germinal centers (GC) in lymphoid organs and tissues. Here B cells undergo multiple rounds of antigen-driven proliferation, somatic hyper-mutation (SHM) of Immunoglobulin variable (V) regions and selection to identify and expand cells expressing high-affinity antibodies(1, 2), as well as undergoing class-switching and differentiation into plasma or memory cells. The formation and evolution of GCs during an immune response is therefore central in determining the durability, affinity and diversity of antibodies.

Although the B cell receptor (BCR) is critical for initial selection of antigen-specific B cells into the GC, and for capture of antigen during affinity maturation, it is becoming increasingly clear that additional receptors on B cells determine the strength and outcome of GC reactions. Most notably, several studies have identified a critical role for Toll-like receptors (TLRs) in promoting strong GC responses (3-5). It has long been known that TLR ligands can be used as effective vaccine adjuvants, and induce outstanding immune responses(5). This property was originally attributed to TLRs on dendritic cells (DCs), but recent studies have demonstrated that TLR signaling in B cells is also required for effective antibody responses. These studies indicate that TLR signaling in these 2 cell types perform distinct functions; whereas TLR signaling in DCs determines the magnitude of the GC reaction and the overall levels of antibody produced after vaccination, B cell TLR signaling promotes affinity maturation, class switching and generation of memory B cells (6). Furthermore, the contribution of B cell TLR signaling to antibody responses is most pronounced when the antigen and TLR ligands are closely associated or covalently linked, consistent with a model in which co-ligation of BCR and TLR synergize for optimal activation of B cells. This model

was originally proposed in the context of autoimmunity, where BCR recognition of nucleic acids or nuclear components promotes delivery of nucleic acids to endosomal TLR7 and TLR9, promoting activation of autoreactive cells (7-9). Thus, although TLR stimulation can promote effective B cell responses to pathogens, TLR engagement and signaling must also be regulated to prevent generation of high affinity autoantibodies. The mechanisms by which this is achieved, and how this affects the balance between host defense and autoimmunity, remains poorly understood.

We have recently identified a new role for the vitronectin receptor, αvβ3 integrin, in regulation of TLR signaling in marginal zone (MZ) and B-1 B cells (10). TLR signaling is tightly linked to subcellular localization, which controls access to ligands, and the availability of specific adaptor proteins, which dictate the outcome of TLR signaling (11). As an example, TLR4 signals through NF-κB when engaging ligands at the cell surface, but internalization of TLR4-ligand complexes to endosomes causes engagement of the adaptor TRIF, and activation of IRF3 (12, 13). Likewise, endosomal TLRs, such as TLR7 and TLR9, initially activate NF-kB after engaging ligands, and must traffic to a distinct endo-lysosomal compartment to signal though IRF7 (14). We showed that αvβ3 promotes the intracellular trafficking of TLRs to endosomes competent for IRF7 signaling, and then to lysosomes, where TLR signaling is terminated. Deletion of either αv or β3 integrin subunits from B cells delays TLR trafficking, resulting in increased and prolonged TLR signaling though both NF-κB and IRF7, and increased B cell activation (10). αvβ3 directs TLR trafficking by activation of components of the autophagy pathway, resulting in endosomal recruitment of the Atg8-family member microtubule-associated protein 1A/1B light chains 3B (LC3B). In this setting, LC3 does not form classical autophagosomes, but instead promotes TLR signaling through IRF7, and subsequently directs endosomal fusion with lysosomes. Hence this appears to represent a form of 'non-canonical autophagy', analogous to the LC3-associated phagocytosis (LAP) described in macrophage and DCs(15). We have shown that αvβ3-mediated LC3 recruitment regulates the expansion of autoreactive MZ and B-1 B cells, and αv-CD19 mice have increased

titers of natural antibodies and autoantibodies to dsDNA. However, it is unclear whether this regulatory mechanism is specific to 'innate-like' autoreactive B cell populations such as MZ B cells, or also functions in classical B cell responses to complex foreign antigens.

Here we report that αv integrins play a major role in regulating GC B cell responses to foreign antigens and pathogens associated with TLR ligands and show that deletion of αv from B cells greatly enhances the generation of high affinity, long-lived, B cell responses through specific effects on TLR signaling in GC B cells. TLR signaling in GC B cells activates lipidation of LC3 and re-localization to lysosomes through an αv-dependent mechanism. Disruption of this process leads to increased TLR signaling, expansion of GC, memory and plasma cells, and promotes class switching and somatic hyper-mutation. More importantly, our data indicate that loss of this pathway can enhance long-lived antibody responses to influenza virus. Thus, this study identifies a new role for αv integrins and autophagy components in GC B cells and demonstrates that release of a regulatory mechanism previously associated with limiting autoimmunity can be beneficial in enhancing effective antibody responses to viruses.

Results

Deletion of αv integrins from B cells causes increased GC B cell numbers

To determine whether αvβ3 regulates GC B cell responses, we first investigated GCs that arise spontaneously in the intestine. GC B cells isolated from Peyer's patches (PP) expressed both αv and β3 heterodimers, and surface expression of αvβ3 was several times higher than in non-GC B cells from the same lymphoid tissue (**Figure 1A**), as previously reported by Wang *et al* (16). Spontaneous GC formation in the PP is stimulated by TLR ligands derived from commensal bacteria, and GC B cells purified from PP responded to TLR stimulation by activation of NF-κB. In addition, TLR stimulation of GC B cells caused aggregation and re-localization of LC3, consistent with TLR-mediated activation of autophagy components and fusion of LC3-containing endosomes to lysosomes, as we have previously reported for MZ and B-1 B cells. αv-knockout

PP GC B cells showed increased and prolonged NF-κB activation in response to TLR stimulation (**Figure 1B**) and failed to reorganize LC3 (**Figure 1C,D)**. Deletion of αv from B cells using the CD19-Cre knock-in mouse strain (*Itgav*$^{flox/flox}$*; Cd19*$^{Cre/+}$ mice, referred to as αv-CD19 mice) resulted in an increase in GC B cell frequency in both PP and colon lamina propria compared with littermate control mice (*Itgav*$^{flox/+}$*; Cd19*$^{Cre/+}$ genotype) (**Figure E,F**). Together these data show that GC B cells also mobilize the autophagy component LC3 after TLR stimulation, through a mechanism involving αv integrin, and deletion of αv results in dysregulated TLR signaling and GC B cell expansion in vivo.

Increased GC B cells in αv-CD19 mice immunized with TLR ligands

To study the role of αv in GC cells in more detail, we immunized αv-CD19 mice and littermate controls with virus-like particles (VLPs) derived from bacteriophage Qβ capsid proteins(17). These Qβ VLPs induce strong GC reactions that are dependent on B cell TLR7 signaling in response to ssRNAs contained within the VLP (17, 18). We first measured expansion of VLP-specific GC B cells, making use of fluorescent Qβ-VLPs. VLP+ B cells were present at very low frequency in non-immunized mice, but could be readily detected in spleen and peritoneal-draining LNs after immunization (**Figure 2A**). VLP+ B cells were present at higher frequency in LNs from αv-CD19 mice than from littermate controls after immunization. Furthermore, a higher proportion of VLP+ B cells expressed GC markers (PNA+, FAS+, GL7+) compared with control mice (**Figure 2B, C**). A similar increase in VLP+ GCs cells was observed in the spleen of αv-CD19 mice, although the overall frequency of VLP+ B cells was not affected (**Figure 2C)**. We reasoned that the increase in GC cells could be due to either increased recruitment to the GC pool, or increased proliferation once in the GC and to distinguish these possibilities, we measured GC B cell proliferation by incorporation of the nucleoside analog BromodeoxyUridine (BrdU). A higher proportion of BrdU+ VLP-specific B cells were seen in αv-CD19 mice than in controls (**Figure 2D**), suggesting that increased proliferation was responsible for the higher numbers of GC B cells in αv-CD19 mice.

GC B cell proliferation and expansion occurs primarily in the dark zone, and we also observed an increase in VLP-specific cells expressing markers consistent with GC dark zone (DZ) occupancy in αv-CD19 mice (**Figure 2E**), further supporting this explanation.

Loss of αv confers competitive advantage to GC cells

To test whether the effects of αv deletion on GC B cell proliferation were cell-intrinsic, we generated mixed BM chimeras between αv-CD19 and wild-type congenic mice (B6.SJL) (at 1:1 ratio; **Figure 3A**). Chimeras were immunized with VLPs, and relative numbers of αv-deficient and congenic cells in B cell compartments measured (**Figure 3B**). The relative proportion of αv-deficient B cells in the total B cell population was similar to that in other hematopoietic cells, indicating that αv-deletion did not greatly affect differentiation into B cells. However, the proportion of αv-deficient B cells in the VLP+ population was significantly higher than in the total B cell pool, and was further increased in the VLP+ GC population, where in some cases over 90% of VLP+ GC cells were derived from αv-deficient bone marrow (**Figure 3C)**. Selection into the VLP+ and GC pools was not seen in equivalent chimeras between control cells (which carry the same CD19-Cre allele as αv-CD19 mice) and wild-type congenic cells (Con-WT) (**Figs 3B and C**). Based on these data we concluded that deletion of αv provides a competitive advantage to GC B cells, and that expansion of GC B cells in αv-CD19 mice was due to cell-intrinsic effects of αv deletion on GC B cells.

αv integrins activate autophagy components and regulate TLR signaling in GC B cells

To determine whether αv directly affects GC B cell responses to stimulation, GC B cells from VLP-immunized control and αv-CD19 mice were purified and re-stimulated in vitro. Stimulation of purified GC B cells with either VLPs or the TLR9 agonist CpG DNA induced rapid activation of NF-κB (by 45 minutes), which was transient, declining to close to baseline levels by 120 minutes (**Figure 4A**). Stimulation of GC B cells also resulted in activation of IRF7, which occurred with

slightly slower kinetics than NF-κB, remaining elevated 120 minutes after stimulation with VLPs (**Figure 4A**). Similar to our previous findings in MZ B cells(10), TLR stimulation of GC B cells triggered lipidation of the autophagy component LC3 (**Figure 4B**) and reorganization of LC3 from a distributed pattern throughout the cytosol, to aggregates at the center of the cell (**Figure 4C,D**), which we have shown correspond to LAMP2+ lysosmes (10). Consistent with a role for LC3 in lysosomal trafficking, levels of the cargo receptor p62, which binds LC3 and is degraded after lysosomal fusion, dropped sharply in control GC B cells following TLR stimulation (**Figure 4B**). In αv-deficient GC B cells, NF-κB signaling was increased and prolonged in response to TLR or VLP stimulation, remaining highly elevated 2h after stimulation, while IRF7 activation was delayed **(Figure 4A**). αv-knockout GC B cells also did not show increases in LC3 lipidation (**Figure 4B, Supplementary Figure 1**) and reorganization (**Figure 4C**), or p62 degradation (**Figure 4B, Supplementary Figure 1**). Hence, we concluded that αv regulates TLR signaling in GC B cells, and that this occurs through the autophagy-related mechanism.

Curiously, although non-GC follicular B cells from VLP-immunized mice also respond to stimulation with VLPs and TLR9 agonists, as evidenced by NF-κB activation, they did not show any detectable activation of IRF7, or increase in LC3 lipidation, LC3 reorganization, or degradation of p62 (**Figure 4 E, F, Supplementary Figure 2**). Indeed, non-GC follicular cells expressed much lower levels of LC3 and p62 than GC cells from the same mouse (**Figure 4 B,F**). Furthermore, we did not observe any significant difference between TLR responses in αv-knockout and control non-GC follicular B cells. Based on these results, we conclude that the ability of αv to activate autophagy components following TLR signaling is a specialized property acquired by GC B cells, and that this allows activation of IRF7 in response to TLR ligands, but also regulates the strength and duration of TLR signaling in these cells.

To determine how αv-deletion and altered TLR signaling impacts the activation and expansion of B cells in GCs we examined expression of key genes involved in GC B cell function and differentiation. Expression of genes involved in somatic hypermutation (*Aicda* or AID), plasma

cell differentiation (*Prdm1/* BLIMP) and class-switching to IgG2c (*Tbx21/* T-bet) were all increased in VLP+ GC cells from αv-CD19 mice compared with control cells, whereas genes involved in general GC differentiation (*Myc* and *Bcl6*) were either unchanged or downregulated (**Figure 4G**). Furthermore, these changes in gene expression were observed as early as day 5 after immunization, and sustained at 14 days. Together, these data show that increased GC B cell expansion in αv-CD19 mice are associated with stronger responses to TLR stimulation, and lead to qualitative differences in GC B cell phenotype.

Non-canonical autophagy regulates GC B cell response

To specifically address the role of non-canonical autophagy in GC response we focused on Rubicon, a protein that has recently been described to be required for LC3-associated phagocytosis, a form of non-canonical autophagy, but is not required for macro-autophagy (19). We confirmed that Rubicon was also required for TLR-induced autophagy in B cells, as LC3 lipidation was impaired in Marginal zone (MZ) B cells from Rubicon-knockout mice after stimulation with the TLR9 agonist CpG (**Figure 5A**). Furthermore, B cells from Rubicon knockout mice showed increased proliferation in response to TLR9 and TLR7 ligands **(Figure 5B-C**) compared to control cells, similar to our previous findings with αv-deficient, Atg5-deficient and LC3-deficient B1 and MZ B cells (10). This effect was not seen in follicular B cells and loss of Rubicon did not enhance B cell responses to IgM stimulation **(Figure 5C**), demonstrating that as with αv-deletion, the effects of non-canonical autophagy were specific to stimulation of activated B cell populations by TLR ligands.

To directly address the role of Rubicon in GC B cells we used a competitive assay as outlined in Figure 3. Mixed bone marrow chimeras generated with a 1:1 ratio of Rubicon knockout and wild-type congenic cells were immunized with VLP, and proportions of knockout cells in the VLP-reactive GC and non-GC subsets assessed by FACs. Rubicon deficient B cells were significantly enriched in to VLP+ GC compartment **(Figure 5E),** indicating that loss of Rubicon

provides a competitive advantage to GC B cells, as we have seen with αv-deficient cells. Together these data support our hypothesis that αv regulates GC B cell responses through Rubicon-mediated non-canonical autophagy.

αv-CD19 mice produce higher IgG2c titers in response to TLR ligand adjuvants.

We next analyzed the effects of changes in GC B cells on antibody production in αv-CD19 mice. Titers of serum anti-VLP IgG were increased by approximately 2-fold in αv-CD19 mice compared with controls (**Figure 6A**) following immunization with VLPs. Similar increases were seen in anti-VLP IgG2c in αv-CD19 mice, whereas anti-VLP IgG1 and IgM were not significantly different from controls (**Figure 6A**). Anti-VLP IgG and IgG2c titers were increased in αv-CD19 mice at day 14 and day 21 after immunization, but dropped to similar levels as in control mice as the primary antibody response waned at day 35 and beyond, indicating that αv-deletion affected the magnitude of the primary immune response, but not the duration (**Figure 6B**). Strong antibody responses to Qβ-VLPs have been shown to require TLR signaling in B cells and DCs, which is triggered by ssRNA contained within the VLP binding to TLR7. To confirm that increases in VLP antibody response in αv-CD19 mice were due to effects on TLR signaling, mice were immunized with Qβ-VLPs lacking ssRNA. Both αv-CD19 and control mice mounted antibody responses to these 'empty' VLPs, but levels of anti-VLP IgG and IgG2c were significantly (5-10 fold) lower than titers in mice immunized with ssRNA-containing VLPs, whereas IgG1 titers were unchanged (**Supplementary Figure 3**) as reported previously(18). Importantly, we saw no difference in antibody titers between αv-CD19 and control mice in response to TLR-ligand-free VLPs, demonstrating that the differences in anti-VLP responses in αv-CD19 mice were dependent on TLR signaling.

To determine whether the increases in IgG2c titers in αv-CD19 mice could be explained solely by increased responses to TLR7 signaling, we substituted VLPs for a vaccine-grade

formulation of the TLR7 agonist Imiquimod (Imiquimod-SE), combined with a model protein antigen, Nitro-phenol-haptenated chicken γ-globulin (NP-CG). Similar to our findings with VLP immunization, αv-CD19 mice immunized with NP-CG/ Imiquimod-SE produced higher serum titers of anti-NP IgG2c than control mice (**Figure 6C**). In addition, αv-CD19 mice also produced higher levels of anti-NP IgM and IgG1 than control mice, although these increases were less pronounced than for IgG2c. In our previous study, we showed that αv-CD19 mice produced normal levels of IgG and IgG2c to anti- NP-CG in the presence of an alternative, TLR-independent adjuvant, alum, but IgG2c levels were elevated when the TLR4 ligand LPS was used as an adjuvant (10) **(Figure 6D)**. Together, these data show that the αv-CD19 mice mount stronger primary IgG2c antibody responses to antigens associated with either endosomal (TLR7) or cell surface (TLR4) TLRs, supporting our hypothesis that changes in GC B cell function and increased antibody responses in αv-CD19 mice are due to loss of regulation of TLR signaling.

αv regulates long-lived antibody responses to TLR-ligand adjuvants.

A hallmark of GC reactions is the generation of long-lived plasma cells and memory cells that provide long-term immunity and rapid antibody responses to previously encountered pathogens. To test whether αv integrins affected either of these aspects of the immune response, VLP immunized mice were re-challenged with low doses of VLPs. To focus on reactivation of B cells by antigen alone, and avoid complications from any increased TLR signaling in αv-deficient memory or plasma B cells, we used 'empty' VLPs, lacking ssRNA, for secondary challenge. αv-CD19 mice produced higher titers of anti-VLP IgG than controls 7d after re-challenge (**Figure 7A**). As we had observed for primary responses, this increase in IgG was predominantly associated with increases in IgG2c (**Figure 7A**), while anti-VLP IgG1 levels were similar in the two strains (not shown). Memory B cells reside in the spleen and other lymphoid organs, and expand in response to re-exposure to antigen to generate plasma cells or re-enter GC reactions. VLP-specific memory B cells, identified on the basis of VLP, CD38 and IgD staining, were present at

a higher frequency in the spleens of re-challenged αv-CD19 mice than in controls (**Figure 7B**). Long-lived plasma cells in the bone marrow (BM) constitutively produce large amounts of antibody. Consistent with the higher levels of serum anti-VLP antibody, we observed greater numbers of VLP-specific IgG2c antibody-producing cells in the BM of re-challenged αv-CD19 mice than in equivalent control mice (**Figure 7C**). To confirm that these increased memory responses in αv-CD19 mice required TLR signaling, we again made use of the model antigen NP-CG, with either TLR-ligand (Imiquimod-SE and LPS) or TLR-independent (Alum) adjuvants. αv-CD19 mice immunized with NP-CG in the presence of TLR ligand adjuvants and re-challenged with NP-CG alone had higher numbers of bone marrow anti-NP antibody producing cells, and higher serum titers of Anti-NP IgG antibody (**Figure 7D, E**). In contrast, memory responses in αv-CD19 mice immunized with NP-CG in alum adjuvant were no different from those in controls (**Figure 7E**). Hence, loss of αv-mediated regulation of TLR signaling affects the generation of memory and plasma cells, consistent with the expansion of GC B cells and increased expression of genes associated with plasma cell differentiation in αv-CD19 mice.

Deletion of αv promotes somatic hyper-mutation and high affinity antibody responses.

A second critical function of GC reactions is to provide antibody diversity and select high-affinity antibodies through successive rounds of immunoglobulin mutation and selection. The affinity of polyclonal serum antibodies to the hapten NP can be assessed by ELISA using NP_{30}- and NP_4-conjugated BSA to measure total and high affinity Igs respectively. The ratio of serum IgG2c measured using NP_4 vs NP_{30} (i.e. the ratio of high to low affinity antibody) was significantly higher in NP-CG/ Imiquimod-SE immunized αv-CD19 mice than in littermate controls (**Figure 8A**). Similar increases in Ig affinity were seen in mice immunized with NP-CG combined with a different TLR adjuvant, LPS, but not in mice immunized with NP-CG in alum (**Figure 8B**). Notably, increased affinity was only seen for the IgG2c isotype, and not for IgG1, consistent with ability of TLR signaling to promote both affinity maturation and IgG2c-class switching, and the role of AID

in both processes. The increased high affinity antibodies, expansion of GC B cells and expression of higher levels of AID (*Aicd* gene) in αv-CD19 mice suggested that αv-knockout GC cells undergo increased somatic hyper-mutation compared with controls. To test this hypothesis, VLP+ GC cells were sorted from αv-CD19 and control mice 14 d after immunization, and BCR heavy and light chains from individual cells sequenced (20). V_H and V_L sequences were generated from between 49-87 single cells, matched to reference genomic sequences and the number and position of mutations determined. αv-CD19 mice showed a significant increase in mutations in IgG_H compared with littermate control mice (**Figure 8C,D**).

Deletion of αv enhances antibody response to influenza virus.

Effective vaccination against many viruses relies on the generation of long-lived high affinity neutralizing antibodies. To examine the effects of increased GC responses in αv-CD19 mice on antibody response to viruses, mice were immunized mice with inactivated Influenza A/PR/8/34 virus (PR/8). αv-CD19 mice produced up to 3-fold greater titers of anti-PR/8 IgG antibodies than littermate control mice (**Figure 9A**). Antibody titers remained elevated over control mice at 56 days after immunization, and after a second immunization, were further increased in αv-CD19 mice compared with controls (**Figure 9B**). Furthermore, as seen in our VLP and TLR ligand adjuvant immunization studies, αv-CD19 mice generated higher numbers of bone marrow anti-PR/8 antibody-producing plasma cells than controls (**Figure 9C**), indicating that deletion of αv promotes increased long-lived antibody responses against influenza virus.

A major target of antibody responses to influenza virus is the viral hemagglutinin (HA). To test whether the increased antibodies produced in αv-CD19 mice were functional and effective against Influenza, serum from mice at day 21 after immunization was tested for hemagglutination inhibition (HAI) activity. Serum from αv-CD19 mice had 4-fold higher HAI than serum from littermate control mice (**Figure 9D**). This correlated with increased titers of IgG antibodies against PR/8 in αv-CD19 mice and as we had seen for VLPs and TLR ligand-associated antigens, this

increase in anti-HA IgG was predominantly due to increases in IgG2c antibody (**Figure 9E**). HA is a major source of antigenic variation in Influenza and accumulation of mutations in antibodies during GC reactions has been shown to broaden their reactivity to different influenza HA epitopes(21). To assess whether increased GC responses in αv-CD19 mice were capable of generating antibodies of broader reactivity, we measured the binding of serum from PR/8-immunized mice to HA from the 2009 pandemic H1N1 strain, Influenza A California/04/2009 (Cal/09). Serum from all αv-CD19 mice tested recognized Cal/09 HA, whereas this was only seen for one (of three) control mice (**Figure 9F**). This increase in Cal/09 HA binding remained after normalization to PR/8-HA binding for each sample **(Figure 9G**), suggesting that Cal/09-HA binding could not simply be explained by a higher level of anti-HA antibodies in αv-CD19 mice. However, to overcome any confounding effects from the lower levels of antibody response in controls, mice were immunized with inactivated PR/8 in combination with a TLR-ligand adjuvant, Imiquimod-SE. Addition of Imiquimod induced more uniform and robust anti-HA responses in control mice (**Figure 9H**). Furthermore, consistent with studies showing that TLR-ligand adjuvants can increase the breadth of anti-HA reactivity during influenza vaccination(22-24), control mice consistently produced Cal/09-HA cross-reactive antibody (**Figure 9I**). However, even in the presence of this strong adjuvant, αv-CD19 mice produced higher levels of anti-PR/8 and anti-Cal/09 HA antibodies (**Figure 9 H,I**), and an increase in the ratio of Cal/09 to PR/8 HA binding, as seen with for immunization without adjuvant. Hence, together these data demonstrate that deletion of αv from B cells causes increased functional antibody responses to immunization with inactivated virus, and moreover, that this response is of greater breadth than in control mice.

The accelerated and increased antibody response to inactivated PR/8 suggested to us that αv-CD19 mice may be protected from viral infection. To test this, we infected αv-CD19 mice and littermate control mice with live PR/8. As shown in **Figure 9K**, the majority of control mice had to be euthanized during the course of infection, due to excessive weight loss or other pathology. In contrast, almost all αv-CD19 mice survived infection and regained any weight loss

by 8-9 days post infection. Supporting a role for increased antibody responses in increased protection, αv-CD19 mice had clearly detectable levels of class switched IgG2c anti-HA antibody 7 days after infection, whereas these antibodies were undetectable in surviving control mice at the same time point **(Figure 9L**). Titres of IgG1 were observed in both αv-CD19 mice and controls.

Discussion

Although the role of B cell TLRs in promoting effective immunity is increasingly appreciated, the factors that impact TLR signaling in these cells, and how these affect immune responses, remain poorly understood. Here we describe a new mechanism of regulation of TLR signaling in GC B cells mediated by αv integrins. We show that disruption of this regulatory mechanism by deletion of αv in B cells enhances responses to antigens containing TLR ligands and influenza virus, causing increases in GC B cell expansion, affinity maturation and class switching to IgG2c, and promoting generation of memory and plasma B cells. Our results establish the concept that increasing TLR signaling in B cells is sufficient to promote GC B cell development and differentiation, leading to stronger, high-affinity, long-lived antibody responses that is relevant for response to viruses. Furthermore, we show that this αv-mediated regulatory pathway is associated with GC B cell-specific activation of the autophagy protein LC3, identifying a potential new regulatory role for autophagy components in GC B cells.

Previous studies using genetic targeting of individual TLRs or the TLR signaling adaptor Myd88 have shown that disruption of TLR signaling in B cells causes loss of class-switching, affinity maturation and generation of memory cells (4, 18). Our findings that αv-deletion in B cells increases these responses is therefore consistent with effects on B cell TLR signaling. Furthermore, our data provide an important complement to these earlier studies, establishing that increased TLR signaling in GC cells alone is sufficient to increase immune responses. The ability of GC B cells to signal though TLRs is thought to be particularly important in antiviral immunity, allowing vigorous responses to viral nucleic acids (18, 25, 26). In this context, it is curious that a

number of viruses bind αvβ3 directly to promote their internalization, and αvβ3 has been proposed to function as an innate immune receptor for Herpes Simplex Virus(27). It is therefore possible that the αv-autophagy pathway that we describe is activated by viral engagement of αvβ3, and plays an important role in antiviral immunity, and this is an active ongoing area of study. However, αvβ3 also serves as a phagocytic receptor for apoptotic cells and cellular debris (28, 29), which are known sources of self-antigen that can promote autoimmune disease. We showed previously that deletion of αv from B cells results in the expansion of autoreactive MZ and B-1 B cells, and that αv-CD19 mice have higher titers of autoreactive natural antibodies and autoantibodies to dsDNA (10). We therefore hypothesize that a major role for the αv-autophagy pathway is to regulate responses to self-derived nucleic acids and other TLR ligands, limiting B cell TLR signaling to prevent generation of high affinity, class-switched antibodies from apoptotic material internalized through αv integrins. Here, we show that this mechanism of autoimmune regulation also affects potentially protective responses to foreign antigens and that release of this regulatory mechanism enhances generation of high affinity IgG2c antibodies to TLR-associated antigens through effects on GC B cells.

Based on the effects of αv-deletion on TLR signaling pathways and TLR-dependent functions, we conclude that the phenotype of αv-CD19 mice is primarily due to loss of regulation of TLR signaling. Furthermore, based on the high expression of αvβ3 in GC B cells, and the observation that $\beta3^{-/-}$ B cells also show increased TLR signaling (10), it is likely that the αvβ3 is the integrin heterodimer responsible. β3 has previously been implicated in GC B function, and B cell-specific $\beta3^{-/-}$ mice (generated by bone marrow chimera) also show increased numbers of spontaneous intestinal GC cells, closely mirroring our results (16). In this previous study, the authors speculated that αvβ3 may mediate adhesion or migration of GC B cells. Although we cannot exclude contributions of αv integrins in GC B cell migration (as has been shown for T cells (30, 31)), or other roles such as activation of TGF-β (30, 32), the lack of effect of αv-deletion on B cell responses to immunization with the TLR-independent adjuvant alum strongly argue for our

proposed role for αv in TLR signaling and against a critical role for these integrins in other functions of B cells.

αvβ3 regulates TLR signaling by activating lipidation of the autophagy component LC3b, and promoting recruitment of LC3b to TLR-containing endosomes (10). LC3b recruitment initially allows TLRs to signal *via* IRF7, but subsequently promotes the fusion of TLR-containing endosomes with the lysosome, terminating signaling. As we show here, deletion of αv severely inhibits this process in GC B cells, resulting in increased and prolonged TLR signaling. Although this process involves components of the autophagy machinery, we do not believe it constitutes 'canonical' autophagy (also termed macro-autophagy) as we see no evidence of the formation of archetypal double-membrane autophagosomes (10); instead the involvement of Rubicon in this process indicates that it occurs through a non-canonical pathway, similar to the involvement of LC3 in phagocytosis(15, 19). Signaling in non-GC follicular B cells does not appear to be regulated by through this αv-autophagy mechanism, and expression of αvβ3, LC3 and p62 are all reduced or absent in these cells. Therefore, the ability to activate this αv-autophagy regulatory pathway appears to be acquired by B cells as they differentiate in the GC and upregulate TLR signaling machinery. A recent study showed that GC B cells switch from canonical to non-canonical pathways of autophagy activation during viral infection, although the outcome of this change was unclear (33). Our data are in agreement with this and provide insight into the role for non-canonical autophagy in directing TLR signaling to IRF7 and promoting delivery of internalized ligands to lysosomes (which may promote IRF7 signaling/ IFN production and antigen presentation respectively).

Although we focus here on the effects on TLR signaling, it is likely that αv-mediated non-canonical autophagy has additional roles in GC B cells, such as antigen presentation, as has been proposed for LC3-associated autophagy. Both canonical and non-canonical autophagy are involved in many other processes in B cells, including responding to increased energy demands during rapid cell division or unfolded protein responses during antibody production. Disruption of

autophagy components required for both canonical and non-canonical autophagy in B cells results in more severe phenotypes than we see in αv-CD19 mice, including marked defects in memory and plasma cell responses (34, 35). Dissecting these complex roles for the fundamental process of autophagy will therefore require further identification and study of specific activators of the autophagy machinery, such as αv.

The induction of memory B cells and long-lived plasma cells by vaccines is central for their ability to provide long-term protection(36, 37). Furthermore, promoting B cell somatic hyper-mutation to generate antibodies with greater affinity or breadth is critical for generating effective immunity to pathogens such as viruses that have the capacity to mutate rapidly. This is of particular importance in generating effective neutralizing antibodies to viruses, as emerging evidence from studies of HIV and influenza suggest that effective neutralizing antibodies can require a large number of mutations and potentially several rounds of affinity maturation in the GC. We show here that modulating TLR signaling through the αv-autophagy pathway can promote mutations in antibody sequences in GC B cells, increasing antibody affinity, as well as enhance the generation of long-lived plasma cell response against both VLPs and intact influenza virus. In addition, our results show that increased SHM due to loss of αv on B cells could be effective in generating cross-reactive antibodies against different HA subtypes and we are investigating this in more detail in ongoing studies. TLR ligands have already been harnessed as vaccine adjuvants and are important for immune responses to inactivated or attenuated vaccines (38, 39). Our data suggest that inhibition of regulatory pathways for TLR signaling, such as αvβ3, would enhance their effectiveness, an attractive prospect as selective agonists and antagonists for αv integrins, such as Cilengitide or antibodies, have been developed and used clinically in other settings(40),(41). In summary, we have identified a new mechanism of regulation of GC B cell response by αv integrins and autophagy proteins and this work, together with other recent studies, points to B cell TLR signaling as an important and distinct target for promoting high-affinity long-lived antibody responses to viral antigens.

Experimental Procedure

Mice

αv-CD19 were generated as previously described(10) and maintained on a mixed C57Bl/6/ 129Ola background. Littermates with a single *Cd19-Cre* allele and *Itgav*-flox alleles were used as controls. As the background strains of these mice differ at their Igh-1 loci, and in their ability to make IgG2a vs IgG2c (42), for immunization experiments mice were matched by Igh-1 genotype (all were Igh-1 a/b). αv-CD19 mice backcrossed to C57Bl/6 background (10 generations) were used for all influenza immunization and challenge experiments. C57Bl/6-background αv-CD19 mice were intercrossed with C57BL/6.SJL congenic mice for generation of bone marrow chimeras. *Rubicon* knockout mice on a C57Bl/6 background (19) were obtained from Dr Jennifer Martinez, NIEHS. Both male and female mice of 8-12 weeks of age were used for experiments. All mice were housed under specific pathogen free conditions at Benaroya Research Institute. μMT mice were bred and maintained at Seattle Children's Research Institute animal facility under specific pathogen free conditions.

Antibodies and reagents

Anti-mouse antibodies used for flow cytometry include: CD95 (Jo2/ BV421 cat no 562633, PE cat no 554258), CD138 (281-2/BV421 cat no 562610), CD4 (RM4-5/BV510 cat no 563106), CXCR4 (2B11/CXCR4/ BV421 cat no 562738) CD38 (90/Percp-CY5.5 cat no 562770), B220 (RA3-6B2/ PE-CY7 cat no 552772), CD11b (M1/70/PE cat no 557397), IgM (R6-60.2/PE cat no 553409, BV510 cat no 747733), IgD (11-26c.2a/BV605 cat no 563003), CD19 (1D3/ BV650 cat no 563235, APC-CY7 cat no 557655, PE-CY7 552854), CD23 (B3B4, PE-CY7 cat no 562825) and Mouse BD Fc block (2.4G2/cat no 553142) were from BD Biosciences. GL7 (GL7/efluor 660 cat no 50-5902-82) and anti-integrin αv antibody (ebioHMA5-1) were from eBioscience. CD86 (GL1, Percp-CY5.5 cat no 105028) and CD73 (Ty/11.8, Perp-CY5.5 cat no 127213) were from Biolegend. Goat anti-rabbit IgG (H+L) Alexa Fluor 546 (cat no A11010), Streptavidin Alexa Fluor-

647 (cat no s32357) and Hoechst 33342 were from Invitrogen Molecular Probes. Type C -CPG-ODN 2395, Type B CPG ODN 1826 and Imiquimod were from Invivogen. Antibody to anti-NFkappa-B p65(D14E12/cat no 8242), anti-LSD1 (C69G12/cat no 2184) and horseradish peroxidase conjugated anti-rabbit IgG were from Cell Signaling Technology. Anti-LC3B anti-β-actin (AC-15/cat no L7543), and LPS (from *E. coli* O55:B5) were from Sigma-Aldrich. Alkaline phosphatase conjugated anti-mouse IgG-AP (cat no 1030-04), anti-mouse IgG2c-AP (cat no 1079-04), anti-mouse IgG1-AP (cat no 1070-04), anti-mouse IgM-AP (cat no 1020-04) and anti-mouse IgG(H+L) (cat no 1010-01) were from Southern Biotech**.** PNA-FITC was from Vector laboratories**.** P62 antibody (cat no 03GP62-C) was from American Research Products. IRF antibody was from Santa Cruz Biotechnology (H-246/ cat no sc9083) Recombinant HA from PR8 or Cal/09 were purchased from Sino, Biologicals. H1N1 PR/8 was purchased from Charles River. Vaccine grade TLR7 ligand adjuvant Imiquimod-SE was from Infectious disease research institute (IDRI), Seattle.

Flow cytometry and cell sorting

Cells were harvested in PBS/ 0.5% BSA/ 2 mM EDTA and splenocytes or bone marrow cells were depleted of red blood cells (ACK lysis buffer, GIBCO). Single cell suspensions blocked with Fc Block (BD Biosciences) and stained with fluorochrome tagged antibodies for surface markers (1: 200 dilution) at 4°C for 30 min. For detection of Qβ-specific cells, cells were stained with AlexaFlour 647-labelled Qβ-VLPs together with the antibodies for surface markers. Samples were acquired using LSRII flow cytometer (Becton and Dickinson) and analyzed by FlowJo software (Tree Star Inc.). For sorting of spleen GC and follicular cells, after B cell enrichment with the negative selection cocktail (Stem Cell Technologies), cells were labeled with anti-B220-PE-CY7, anti-CD38-PerCP-CY5.5, anti-CD95-BV421 and anti-PNA-FITC antibodies then sorted with FACS Aria (BD Bioscience).

In vitro proliferation : FACs sorted spleen Marginal Zone and Follicular or peritoneal cavity B1 cells were plated in X-VIVO15 (Lonza) supplemented with 2 mM glutamine, 100U/ml penicillin and 100µg/ml streptomycin, and 50µM 2-β-mercaptoethanol or complete RPMI-1640 (10% fetal bovine serum 2 mM glutamine, 100U/ml penicillin and 100µg/ml streptomycin, and 50µM 2-β-mercaptoethanol) at a density of $3X10^4$ cells per well on 96 well plate and treated with different stimuli: CPG (2), Immiquimod (10µM) and IgM (10µg/ml). After 48 hr cells were pulsed with 1µCi/ well tritiated thymidine ([3H]-TdR) for 18 hr prior to harvest; incorporation was determined by liquid scintillation spectrometry.

In vivo proliferation: Mice were injected with 2µg VLPs i.p and 12 hr before harvest on day 14 injected i.p with 1mg BrdU (BD Bioscience). Cells were then harvested from spleen and lymph nodes and stained for surface antigen as described and processed using an anti-BrdU-FITC kit (BD Biosciences).

BCR sequencing

Single VLP+ GC (CD19+ VLP+PNA+ FAS+ CD38 neg) cells were FACs sorted into 96 well plate using Aria II. BCRs were amplified and sequenced from cDNA of single cells as previously described (20, 43). The numbers of somatic hyper-mutation in both heavy (V_H) and light (V_L) chain sequences in individual cells were calculated after comparison to germline sequence.

BM- transplantations

BM was harvested from femora and tibiae of C57BL/6.SJL (control with CD45.1 congenic marker), αv-CD19 (CD45.2 congenic marker) C57BL/6 (control with CD45.2 congenic marker) mice. Single cell suspension were CD138 depleted (Miltenyi Biotech) and mixed at 50:50 ratio {(control CD45.1: αv-CD19 CD45.2) or (control CD45.1: control45.2)}. $6X10^6$ total BM was injected into lethally irradiated (450cGY X2 doses) µ-MT recipients. Resulting chimeras were bled at 4 weeks

to check chimerism in blood and at 6 weeks immunized with 2μg VLP. Spleen and lymph nodes were harvested for analysis at day 14 after immunization.

Confocal microscopy

FACS-sorted GC B cells, or non-GC follicular cells were seeded on to poly-L-lysine coated glass cover slips (BD Bio-coat) in complete RPMI 1640 and allowed to attach for 1 hour at 37°C. Cells were stimulated with 3μM CpG or 1μg/ml VLPs for the indicated times. After stimulation cells were fixed with 4% PFA for 20 min at room temperature (RT), permeabilized with saponin (0.2% saponin in PBS, 0.03M sucrose, 1% BSA) for 10 min at RT. Non-specific binding in cells was prevented by incubating for 1h at RT with blocking buffer (2% goat serum, 1% BSA, 0.1% cold fish skin gelatin, 0.1% saponin, 0.05% Tween-20 in 0.01M PBS, pH 7.2). Cells were incubated overnight at 4C with s primary antibody (LC3 1:500 dilution) in dilution buffer (PBS, 0.05% Tween-20, 1% BSA, 0.1% saponin). Cells were washed 3 times in dilution buffer (5 min each) and incubated in secondary antibodies (1: 500 dilution) in dilution buffer for 1h at RT and washed 3 times in dilution buffer and twice in PBS. Cell nuclei were stained with Hoechst 33342, and the cover slips were mounted with ProLong Antifade (Invitrogen). Cells were imaged 100x oil objective (aperture 1.4) and Nikon Ti (Eclipse) inverted microscope with Ultraview Spinning Disc (CSU-X1) confocal scanner (Perkin Elmer). Images were captured with an Orca-ER Camera using Volocity (Perkin Elmer). Post-acquisition analysis such as contrast adjustment, deconvolution through iterative restoration and 3D reconstruction were performed using Volocity software. LC3 puncta were quantified by counting 10-50 cells per condition in a blinded manner and defining LC3 staining patterns as as distributed around the cells or as punctate.

ELISA

Immulon 2HB microtiter plates (DYNEX) were coated with with either NP-BSA (Biosearch Technologies) 10 μg/ml, VLPs (2μg/ml), inactivated PR/8 (1μg/ml), recombinant HA from PR/8 or

HA from Cal/09 (0.5μg/ml) in PBS overnight at 4°C. Plates were then washed and blocked for 60 min at 37°C (2% BSA, 2% fetal calf serum, 0.1% Tween-20, 0.02% sodium azide in PBS). Serum samples were initially diluted at (1:200) in 50% block, and then loaded onto the plate as a 6-point series of 4-fold dilutions. After incubation for 60-120min at 37°C, bound antibody was detected using alkaline phosphatase-conjugated goat anti-mouse IgM or IgG (Southern Biotech) diluted in blocking buffer for 60 min at 37°C. Secondary antibodies were detected by using disodium p-nitrophenyl phosphate substrate (Sigma Aldrich) and absorbance (OD) read at 405 nm. Antibody titres were calculated from comparisons of dilutions required to achieve the same OD, relative to a standard antibody.

ELISPOT

To detect antigen specific long-lived plasma cells in the BM, 96-well filter plates (Millipore) were coated overnight with antigen: VLP 2μg/ml, NP-BSA 10μg/ml in PBS at 4°C. after blocking with RPMI 1640 with 10% FBS for 1 hr , 2 fold dilutions of BM single cell suspension was added to the filter plates starting with 2 $X10^6$ cells /well in RPMI 1640 with 10% FBS and incubated for 12 hr at 37°C**.** Plates were washed with PBS and incubated with AP conjugated anti-mouse IgM , total IgG , IgG1 or IgG2c (Southern Biotechnology) and developed with BCIP/NBT alkaline phosphate substrate kit (Vector laboratories). Plates were washed with water, dried and ELISPOT were counted in each well.

Western Blots

Nuclear extracts were prepared by lysing cells in hypotonic nuclear extraction buffer (1M Hepes, PH7.5, 5M NaCl, 0.5M EDTA PH8, 50% glycerol, 10% Igepal, 10% TritonX100) for 10 min followed by centrifugation at 1500g for 5 min at 4°C to pellet the nuclei and nuclei were resuspended in RIPA buffer. Lysates were centrifuged for 10 min at 4°C at 14000g and supernatant was collected as nuclear fraction. Proteins were quantified by BCA assay (Pierce),

separated by electrophoresis using NuPage-Bis-Tris gels (Invitrogen) and blotted onto PVDF membranes. Non-specific binding was blocked with 5% BSA in TBS-Tween (0.1%) followed by incubation with primary antibodies (1:1000 dilution) overnight at 4°C and secondary antibody horseradish peroxidase conjugated antibodies (1:2000 dilution) for 1 hr at room temperature. Membranes were washed thoroughly with TBS-Tween (0.1%) after antibody incubations and developed using ECL reagents (Millipore). For re-probing blots were stripped for 30 min at 37 °C with Restore PLUS stripping buffer (Thermo Scientific).

Immunizations/ Infection

For experiments using TLR ligands and alum as adjuvants, mice were immunized i.p with NP-haptenated chicken gamma globulin (NP-CG) (Biosearch technologies) 50 μg per mouse in combination with alum (1:1) or LPS (5 μg /mouse) or clinical gradeTLR7 ligand adjuvant Imiquimod-SE (IDRI, Seattle). For VLP experiments, VLP derived from Qβ bacteriophage were kindly provided by Dr. Baidong Hou (Institute of Biophysics, Chinese Academy of Sciences, Beijing) and the production of these particles have been described previously(18). Mice were immunized i.p with 2μg VLPs and sera was collected at indicated time points by sub-mandibular bleeds. For studies with intact virus mice were immunized i.p with 10μg inactivated H1N1 PR/8 influenza virus (Charles River Laboratories). For challenge studies mice were infected intranasally with 1XLD50 H1N1 PR/8 (Charles River Laboratories) diluted in 25 μl PBS.

QPCRs

RNA was isolated from VLP+ GC cells (CD19+ VLP+ PNA+ FAS+) or total VLP+ B cells FACS sorted directly into TRizol-LS (Invitrogen) and converted into cDNA by reverse transcription (Applied Biosystems). Real-time PCR was performed using with SYBR Green using the following primers:

Aicda, 5’- CCTCCTGCTCACTGGACTTC-3’ (forward) and

5’-GGCTGAGGTTAGGGTTCCAT-3’(reverse);

Tbx-21,5’-GGTGTCTGGGAAGCTGAGAG-3’(forward)and

5’-CCACATCCACAAACATCCTG-3’ (reverse);

Bcl6,5’-TCGTGAGGTCGTGGAGAAC-3’(forward)and

5’-AGAGAAGAGGAAGGTGCTGAG-3’(reverse);

Prdm1, 5’-TGCGGAGAGGCTCCACTA-3’(forward) and

5’- TGGGTTGCTTTCCGTTTG-3’(reverse);

Myc,5’-TCTCCACTCACCAGCACAACTACG-3’ (forward) and

5’- ATCTGCTTCAGGACCCT-3’ (reverse);

Actb,5’-GCCCATCTACGAGGGCTATG-3’(forward)and

5’- CTCAGCTGTGGTGGTGAAGC-3’ (reverse)

Statistics

All statistics tests used are indicated in the relevant figure legends. Statistical analysis was performed using GraphPad Prism, using multiple testing corrections where appropriate. A *p* value less than 0.05 was considered significant.

Study Approval

All animal experiments were approved by following institutional review by the Animal Care and Use Committees at Benaroya Research Institute and Seattle Children’s Hospital Research Institute, and performed under local and national guidelines for animal care.

Acknowledgements

We thank all members of the Acharya, Lacy-Hulbert, Stuart and Rawlings labs for assistance and advice on this project. This work was supported by NIH grant DK093695 (A.L.-H.).

Author Contributions

F.R. and M.A. designed and performed experiments. Additional expertise and assistance in experimental design, execution and analysis were provided by S.S, T.A., G.M., S.D., S.J. and D.R. (Bone Marrow Chimeras and B Cell Receptor Sequencing). M.O. and E.G. provided reagents and advised on immunization and influenza infection experiments. M.A., A.L-H and L.M.S. designed and conceived the study and wrote the paper.

Figure Legends

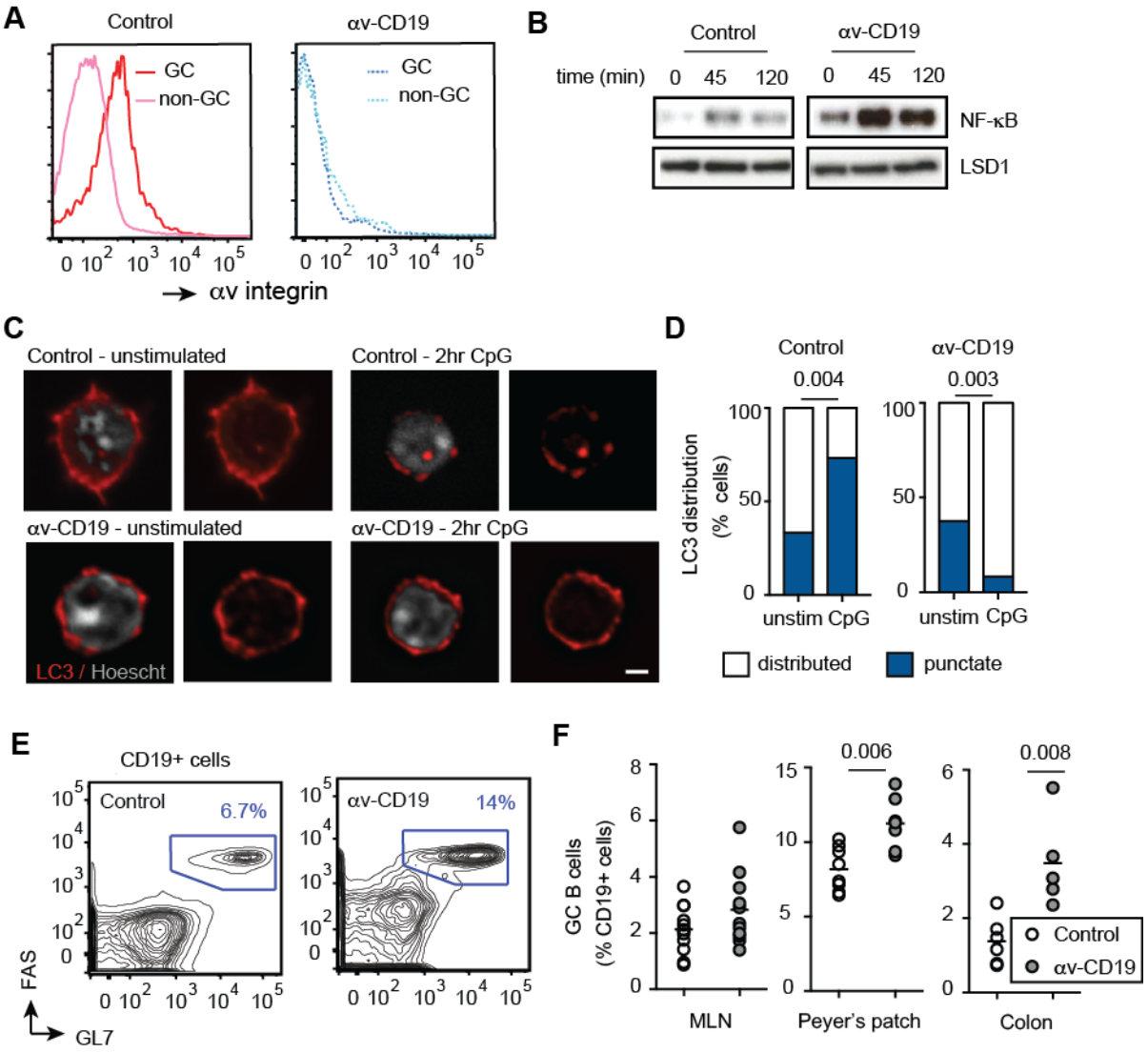

Figure 1: Increased GC B cells in αv-CD19 mice. (A) Histograms show staining for αv on CD19+ cells from control mice (solid line) or αv-CD19 mice (dotted). **(B)** Western blot analysis of NF-κB p65 in nuclear fractions from FACs-sorted Peyer's patch (PP) GC cells from control and αv-CD19 mice stimulated in vitro with CpG for the indicated time (mins). Also shown is the staining for LSD1 to confirm equal loading of nuclear protein. **(C)** Confocal microscopy of FACs-sorted PP GC B cells from control and αv-CD19 mice, with or without in vitro stimulation with 2μM CpG DNA for 2hrs. Cells are stained for LC3b (red) or nuclear DNA (Hoescht, White). Images show representative examples of distributed LC3 expression (unstimulated control and αv-CD19) and punctate expression (CpG-treated control). Scale bar, 2.5μm. **(D)** Proportions of cells undergoing

LC3 reorganization, based on counting of at least 30 cells/ condition. *P*-values are shown (Pearson's chi-square test). **(E)** Representative FACS plots of cells from PP of control and αv-CD19 mice, gated on CD19+ B cells and stained with FAS/ GL7. Gates used for identification of GC B cells, and frequency of GC B cells are shown. **(F)** Quantification of frequency of GC B cells in mesenteric lymph nodes (MLN), PP and colon lamina propria in control and αv-CD19 mice. GC B cells were gated as CD19+ GL7+ FAS+ cells as in **(E).** Each point represents an individual mouse and at least 5 mice were analyzed for in each group. *P* values <0.05 are shown (student's t-test). For all data shown, similar results were seen in at 3 independent experiment.

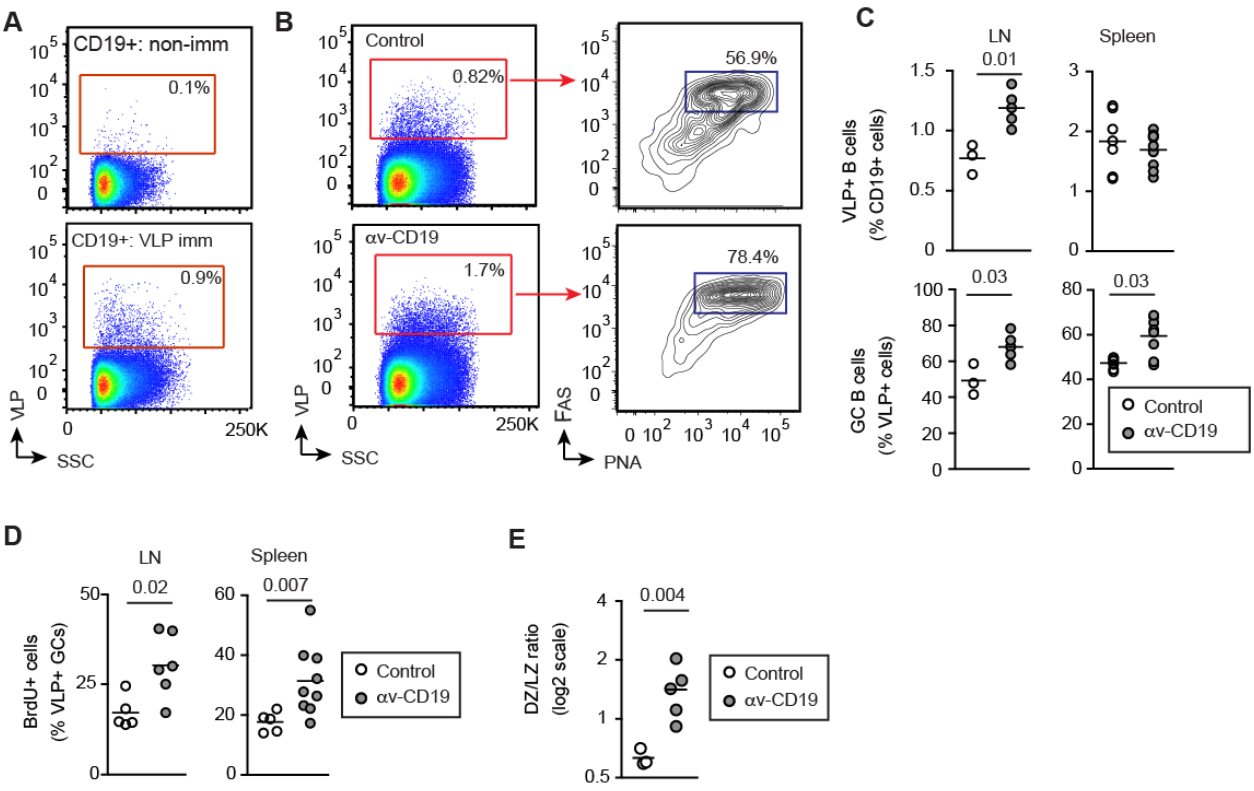

Figure 2: Increased GC B cells in αv-CD19 mice immunized with TLR ligands. (A) FACs plots of cells from LNs from VLP immunized and non-immunized mice stained with fluorescent VLPs, showing VLP+ cells in CD19+ gate. Gating strategy for VLP-specific B cells based on non-immunized mice is shown. **(B)** Representative FACs analysis of VLP+ cells from mediastinal and abdominal LNs of control and αv-CD19 mice 14 days after immunization with 2μg VLPs. Left panels are gated on CD19+ cells, and show VLP+ populations. Right panels show GC B cells (PNA+ FAS+ cells) within the CD19+ VLP+ gate. **(C)** Quantification of VLP+ cells and VLP+ GC cells in VLP-immunized control and αv-CD19 mice. Each point represents a single mouse, bars show mean. **(D)** Proportion of LN and spleen VLP+ GC B cells (gated as in **(B)**) from control and αv-CD19 mice immunized with 2μg VLP for 14d, that stain positive for BrDU 12h after BrDU administration. **(E)** VLP-specific GC cells were gated based on expression of markers of Dark Zone (CXCR4+ CD86-low) and Light Zone (CD86+ CXCR4-low). Data show ratio of DZ/ LZ cells in individual mice, with bars to show the mean. In all cases, *p*-values < 0.05 are shown (Mann-

Whitney-Wilcoxon test). For all data shown, similar results were seen in at 3 independent experiments.

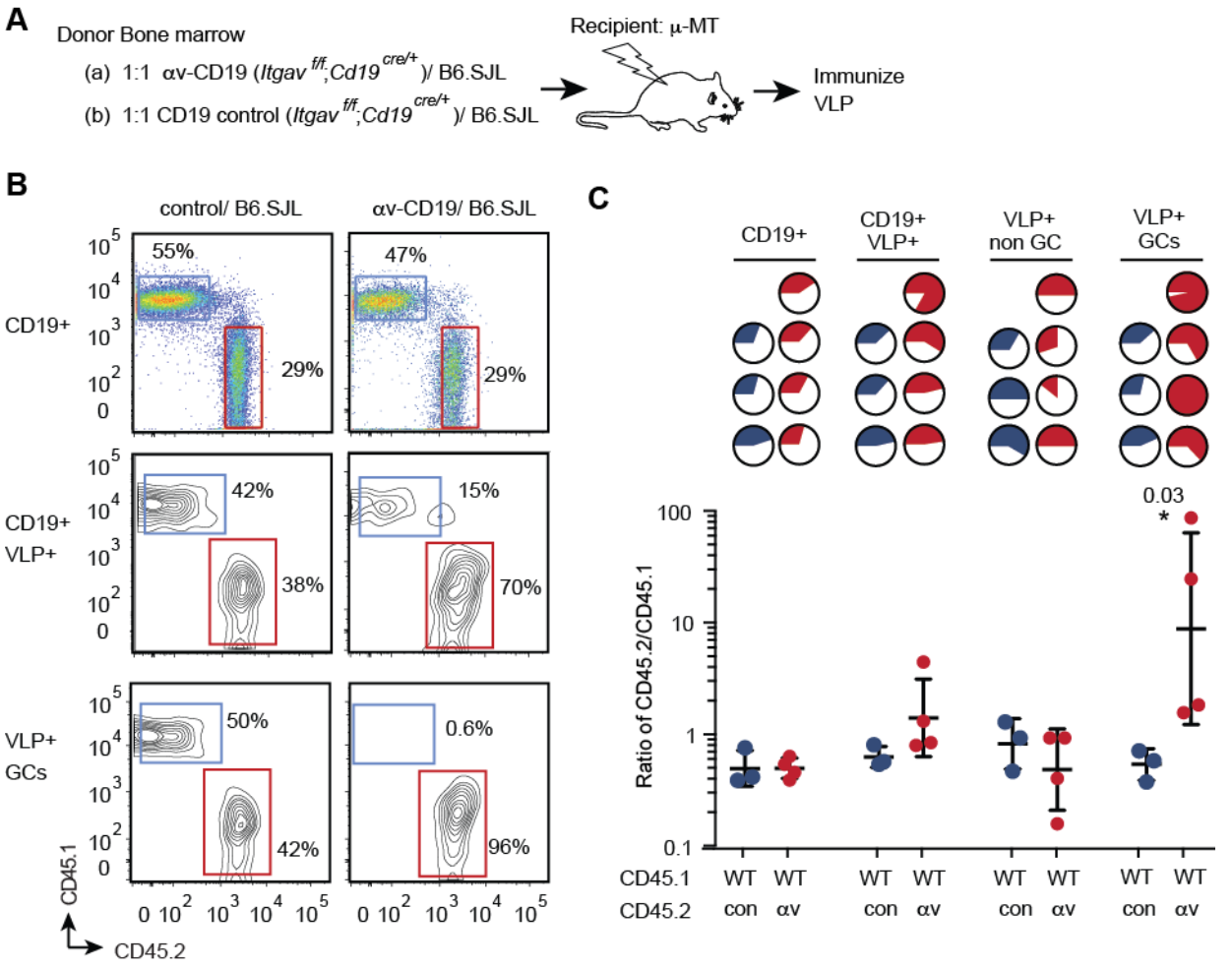

Figure 3: Loss of αv confers competitive advantage to GC cells. (A) Schematic for the experimental plan**.** CD138-depleted BM cells from congenically marked CD45.1 mice (B6.SJL) were mixed 1:1 with BM cells from CD45.2 αv-CD19 mice and injected into irradiated μ-MT mice to generate mixed bone marrow chimeras. Control chimeras were generated with 1:1 mix of B6.SJL BM and CD45.2 control CD19-Cre BM cells. 6 Weeks after reconstitution mice were immunized with 2μg VLP and harvested at day 14 for analysis of antigen-specific B cells by FACS. **(B)** Representative FACS panels for analysis of composition of CD45.1 and CD45.2 cells in CD19+, CD19+ VLP+ or CD19+ VLP+ GC B cell compartments. GC cells were identified as PNA+ FAS+ cells. **(C)** Pie charts in top section of panel show relative proportions of CD45.2+ cells (solid regions of pie charts) in control chimeras (blue) and αv-CD19 chimeras (red) in indicated B cell compartments; each pie chart represents one mouse. Lower panel shows data from all mice in each group expressed as ratio of CD45.2/CD45.1, and geometric mean ± sd. Ratios of

CD45.2/CD45.1 cells for VLP+ non-GC and GC B cells from WT: αv chimeras were compared by Student's t-test of log-transformed data and *p*-value is shown. Data are from 1 representative experiment, with similar results seen in 3 independent experiments.

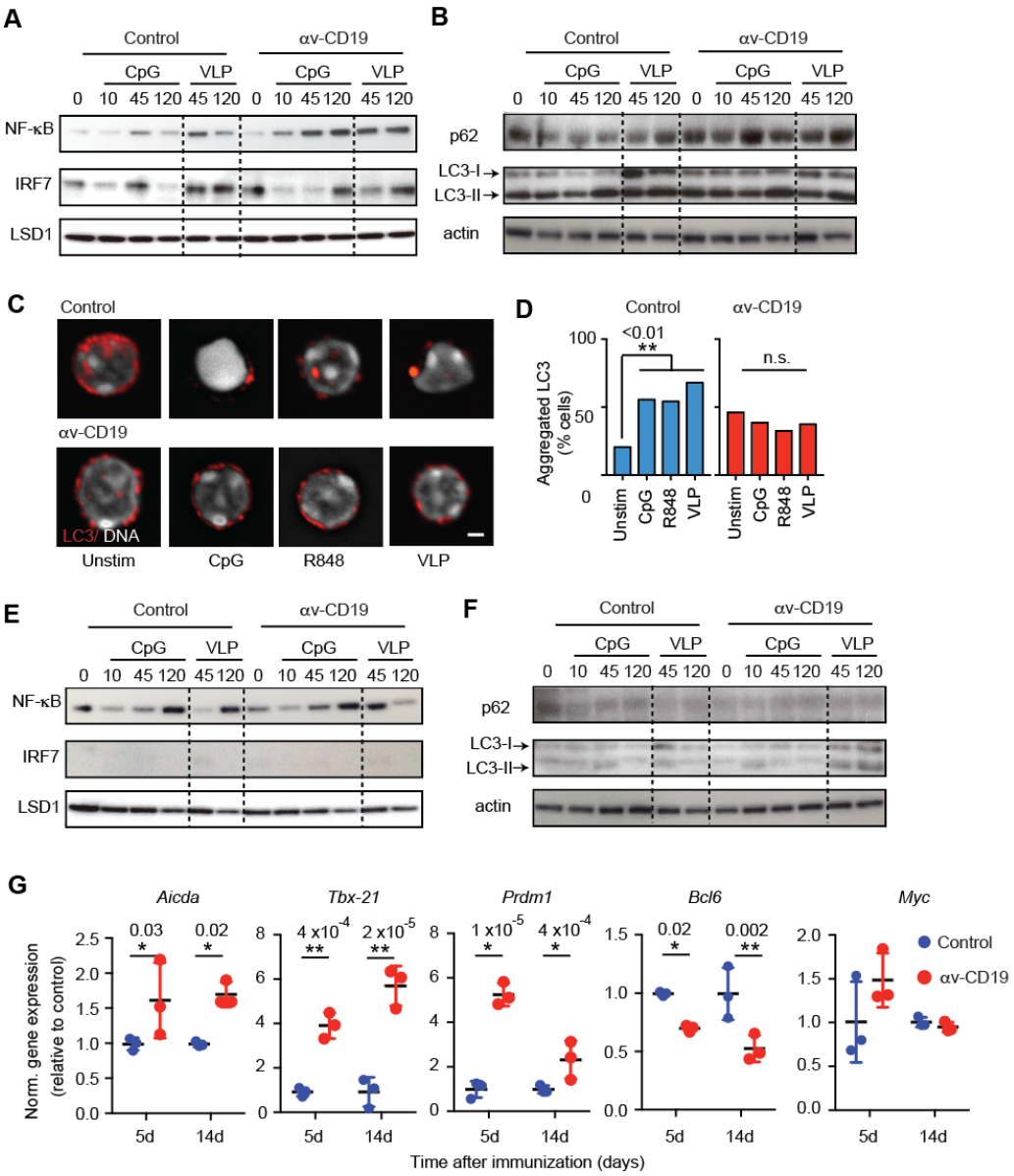

Figure 4: αv regulates TLR signaling in GC B cells through autophagy proteins. (A,B) GC B cells were sorted from spleens of αv-CD19 and control mice 14 days after immunization with VLP, and re-stimulated in vitro with CpG DNA or VLP for the indicated time (mins). Western blots show NF-κB p65 and IRF7 in nuclear fractions **(A),** or p62 and LC3b in whole cell lysates **(B)**. Also shown are staining of LSD1 or actin to confirm equivalent protein loading in nuclear fraction and whole cell lysates respectively. These were performed on the same blot, except in the case of LC3-II where actin staining is from aliquots of the same samples run on parallel gels contemporaneously. **(C)** Confocal images of sorted primary GC B cells (as in **(A-B)**), treated with

CpG DNA, R848 or VLP for 2 hr and stained for LC3 and Hoescht. **(D)** Quantification of LC3 reorganization after stimulation with indicated TLR ligands. Data are based on analysis of at least 30 cells/ condition. *p*-values <0.01 (Pearson's chi-square test) are shown and indicated by **. **(E,F)** FACs-sorted non-GC follicular B cells from spleens of VLP-immunized αv-CD19 and control mice analyzed as in **(A)** and **(B)**. **(G)** Expression of indicated genes measured by QRT-PCR in RNA from FACs-sorted VLP-specific GC cells, isolated 5 or 14 days after immunization with 2μg VLPs. Data from individual mice are shown, with mean ± sd. *p*-values < 0.05 (Mann-Whitney-Wilcoxon test) are shown and indicated by * ($p < 0.05$) or ** ($p < 0.005$). Data are all from one representative experiment of at least 3 independent experiments (2 experiments for p62 blots) in which similar results were seen.

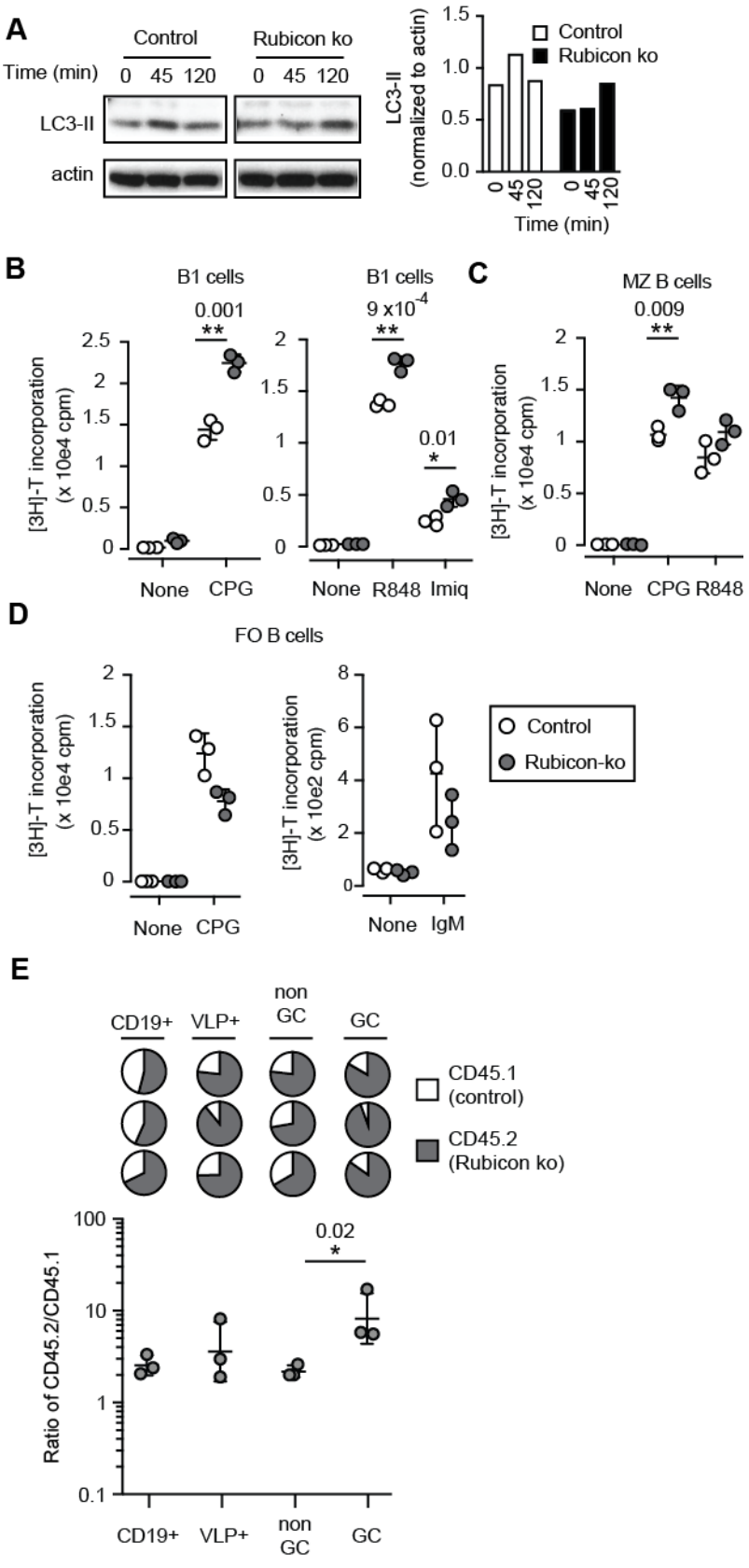

Figure 5: Rubicon-mediated non-canonical autophagy regulates B cell TLR responses. (A)

MZ B cells from Rubicon knockout and control mice were stimulated in vitro with CpG DNA for

the indicated time (mins). Western blots show LC3b and actin in whole cell lysates. Histogram shows quantification of LC3-II normalized to actin for this blot. Similar results were seen in 3 independent experiments. **(B-D)** Proliferation of peritoneal B1 B cells **(B)**, sorted spleen marginal zone (MZ) B cells **(C)** and spleen follicular (FO) B cells **(D)** from Rubicon-knockout and control mice after stimulation with TLR ligands (CpG DNA, R848 and Imiquimod) or anti-IgM. Proliferation was measured by [^{3}H]-thymidine incorporation and is expressed as mean ± sd for 3 independent cultures. *p*-values < 0.05 (Student's t-test) are shown and indicated by * ($p < 0.05$) or ** ($p < 0.01$). Similar results were seen in 3 independent experiments. **(E)** Mixed bone marrow chimeras between control C57B6.SJL congenic mice and Rubicon knockout mice (CD45.2) were generated and used to assess competitive recruitment to GC compartment as described in Fig. 3. Pie charts show relative proportions of CD45.2+ cells (solid regions) in indicated B cell compartments; each pie chart represents one mouse. Lower panel shows data from individual mice expressed as the ratio of CD45.2/CD45.1. Also shown are the geometric mean ± sd. Ratios of CD45.2/CD45.1 cells for VLP+ non-GC and GC B cells were compared by Student's t-test of log-transformed data and *p*-value is shown. Similar results were seen in 2 independent experiments.

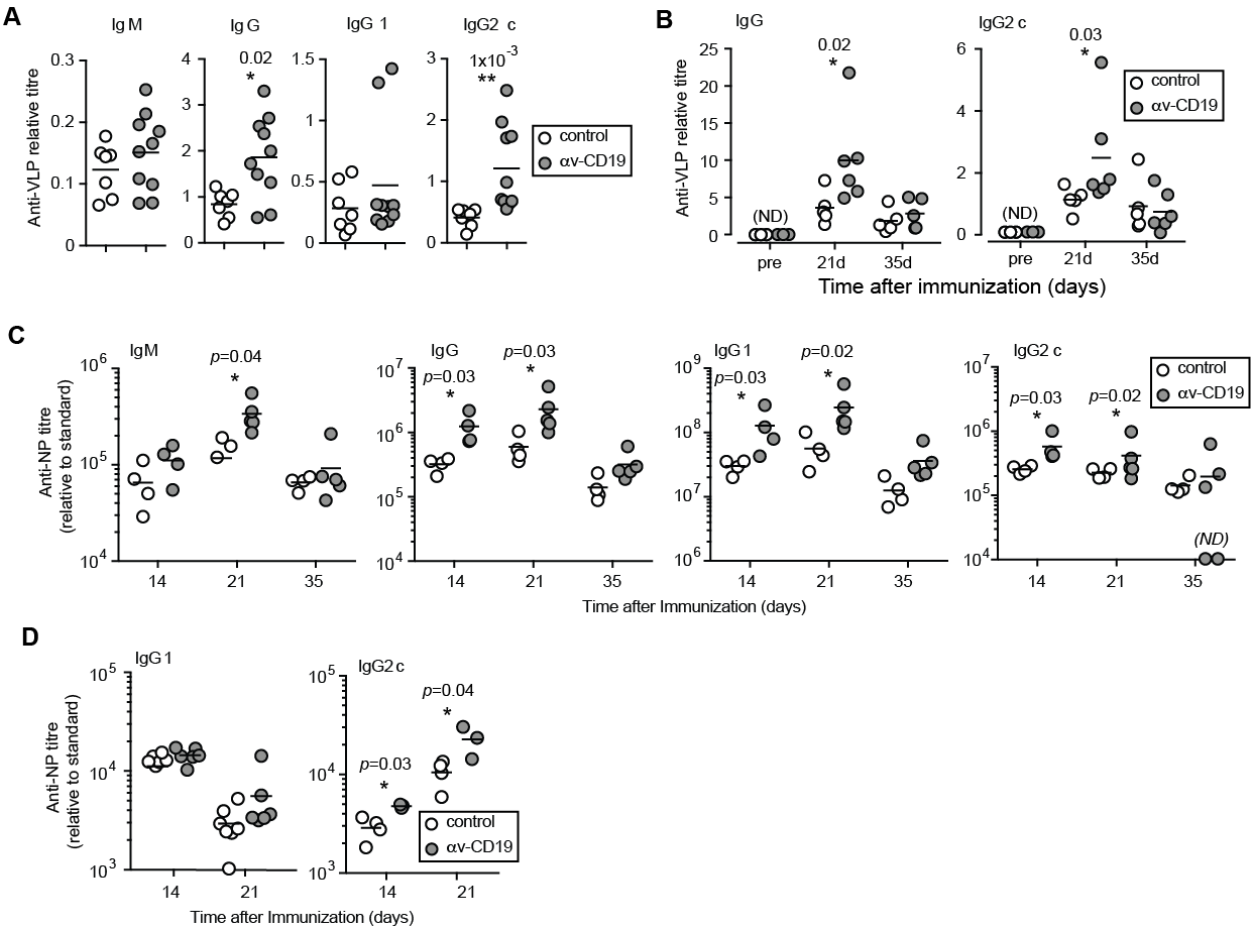

Figure 6: Increased antibody production in αv-CD19 mice. (A-B) Serum anti-VLP antibody titers in control and αv-CD19 mice immunized with 2μg VLPs containing ssRNA measured 14 days after immunization **(A)** or over a time course from pre-immunization (pre) to 35 days **(B)**. VLP specific Abs were not detected (ND) in pre-immunization bleeds. **(C)** Serum anti-NP IgM, IgG, IgG1 and Ig2c titers in control and αv-CD19 mice immunized with NPCG (50μg) combined with TLR7 ligand Imiquimod-SE (10μg). **(D)** Serum anti-NP IgG1 and IgG2c antibody titers in control and αv-CD19 mice immunized with NPCG (50μg) combined with LPS (5μg). All data points represent individual mice with mean shown. *p*-values < 0.05 (Mann-Whitney-Wilcoxon test) are shown and indicated by * ($p < 0.05$) or ** ($p < 0.005$). Samples below the level of detection are indicated as not detected (ND). Similar results were seen in 3 independent experiments.

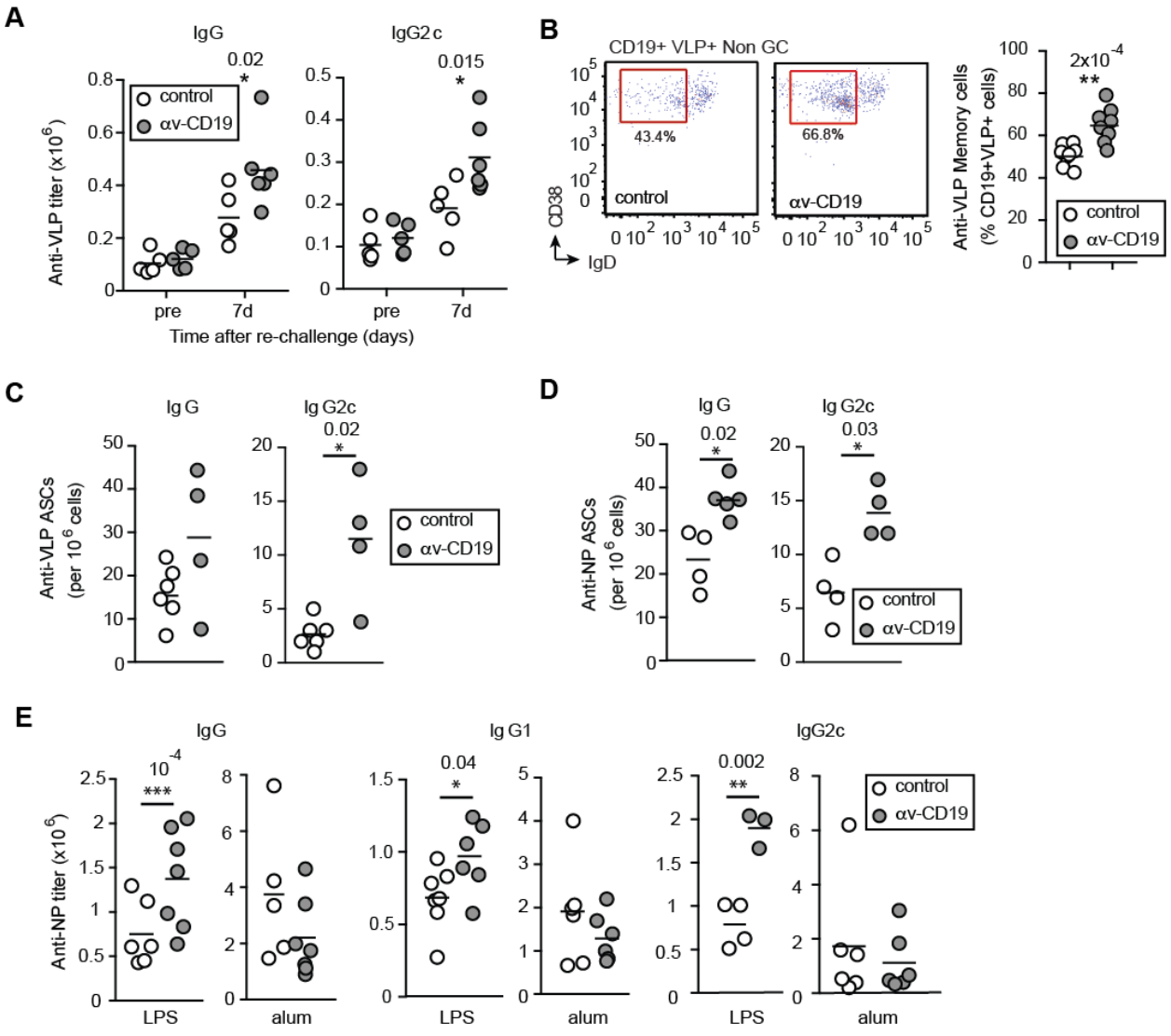

Figure 7: Loss of αv impacts long-lived antibody responses. (A) Serum anti-VLP IgG, and IgG2c titers in control and αv-CD19 mice immunized with 2μg VLPs containing ssRNA, boosted with empty VLP at day 68, and harvested after a further 7 days. **(B)** Frequency of VLP-specific CD38+ IgD low B cells in control and αv-CD19 mice at day 7 post boost as in **(A). (C, D)** Antigen specific plasma cells enumerated by ELISPOT assay on bone marrow cells from control or αv-CD19 mice harvested after immunization and re-challenge with either **(C)** VLPs (2μg) or **(D)** with NPCG with Imiquimod-SE. **(E)** Serum anti-NP IgG, IgG1 and IgG2c titers in control and αv-CD19 mice immunized initially with NPCG with either LPS or alum and boosted at day 42 with NPCG (25μg) alone. All data points represent individual mice with mean shown. *p*-values < 0.05 (Mann-

Whitney-Wilcoxon test) are shown and indicated by * ($p < 0.05$) or ** ($p < 0.005$). Similar results were seen in 3 independent experiments.

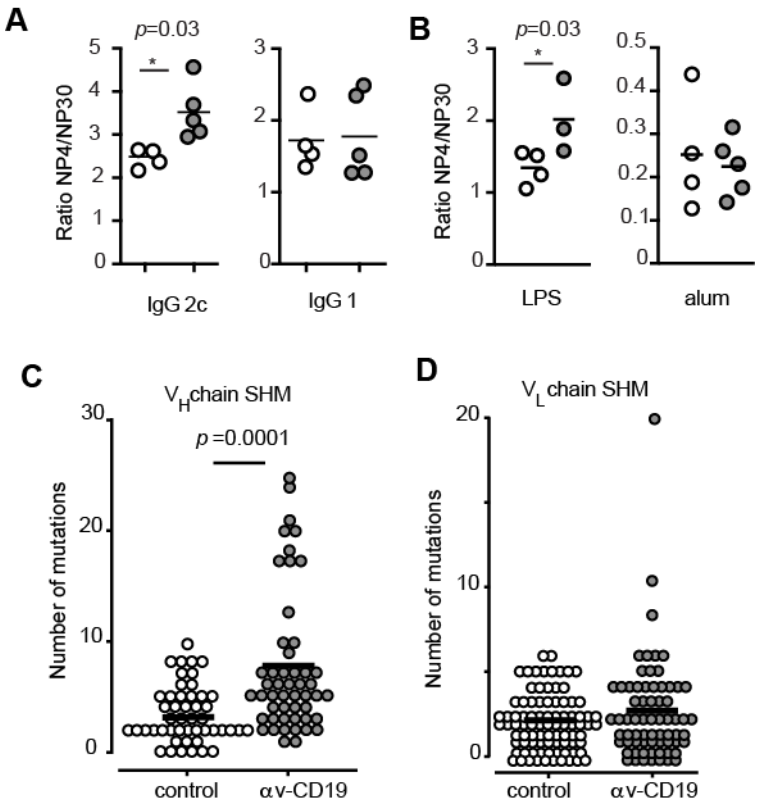

Figure 8: Deletion of αv promotes SHM and affinity maturation of antibodies. (A,B) Affinity maturation of antibodies measured as ratio of anti-NP4/anti-NP30 titers in serum of NP-CG-immunized mice re-challenged with NPCG at day 42 and bled after a further 7 days . Mice were initially immunized with NP-CG and Imiquimod-SE **(A),** or NP-CG in LPS or alum **(B)**. Data points represent individual mice with mean shown. *p*-values < 0.05 (Mann-Whitney-Wilcoxon test) are shown and indicated by *. Similar results were seen in 3 independent experiments. **(C, D)** Point mutations in the IgG heavy chain (V_H) **(C)** or light chain (V_L) **(D)** of individual spleen VLP+ GC B cells 14 days after immunization with 2μg VLPs. Each dot indicates a single cell and line indicates the mean. Mutations were identified by comparing with germline sequences. *p*-values < 0.05 (Mann-Whitney-Wilcoxon test) are shown and indicated by *.

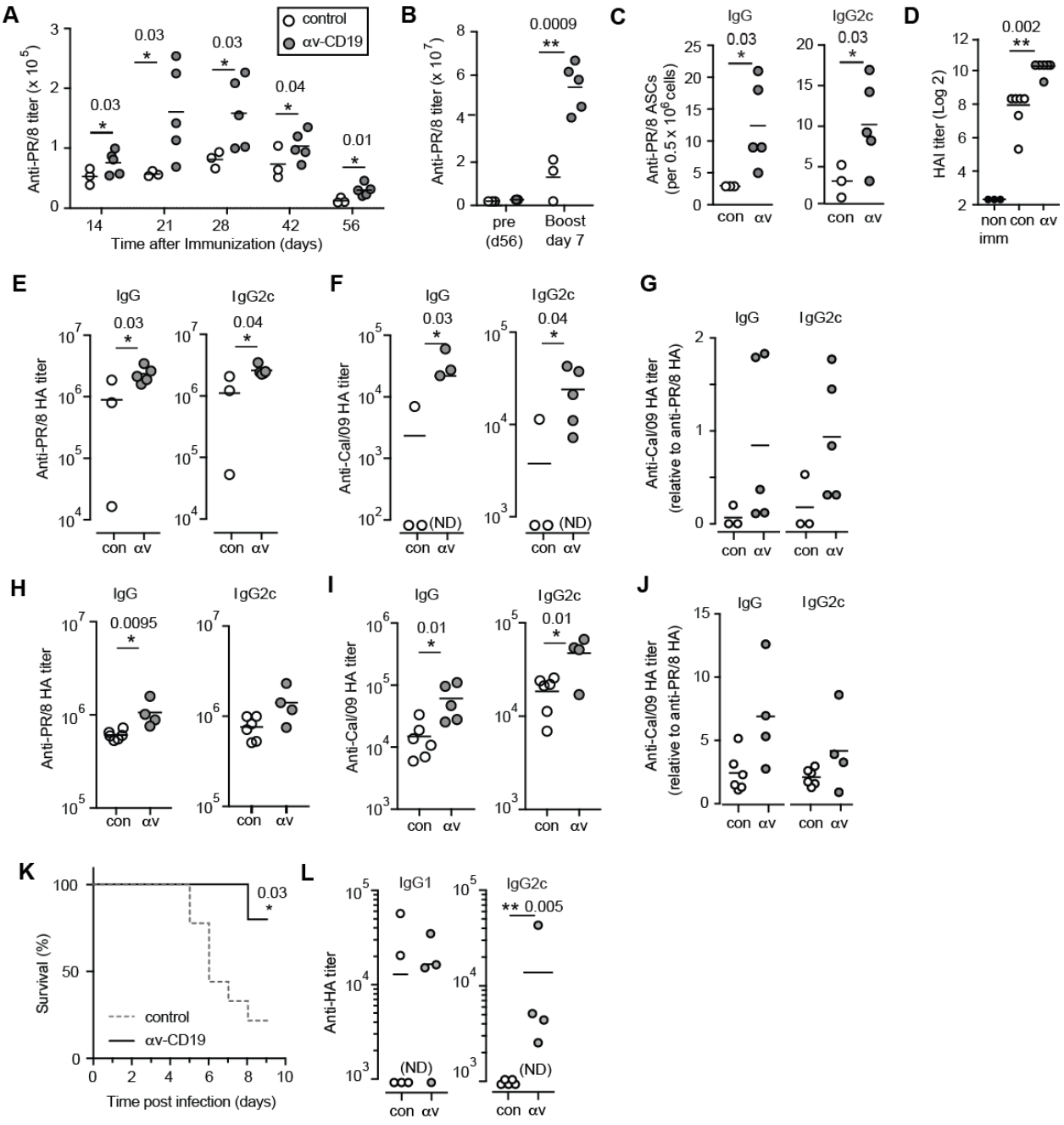

Figure 9: Deletion of αv enhances antibody response to influenza virus. (A,B) Serum anti-PR/8 IgG titers in control and αv-CD19 mice immunized with 10μg of inactivated H1N1 PR/8 **(A)** and **(B)** boosted at day 57 with 5μg inactivated PR/8. **(C)** PR/8 specific plasma cells enumerated by ELISPOT**,** in bone marrow cells from control and αv-CD19 mice harvested at day 7 post boost. **(D)** Hemagglutination inhibition activity in sera from control and αv-CD19 mice at day 21 after PR/8 immunization. **(E, F)** Serum antibody titers against HA from H1N1 PR/8 **(E)** or H1N1 Cal/09

(F) in control and αv-CD19 mice at day 7 post boost with inactivated PR/8. **(G)** anti-Cal/09 HA-titer normalized to anti-PR/8 HA titer**. (H, I)** Serum antibody titers against HA from PR/8 **(H)** or Cal/09 **(I)** in control and αv-CD19 at day 51 after immunization with inactivated PR/8 (10μg) in Imiquimod-SE (10μg). **(J)** Anti-Cal/09 HA-titer normalized to anti-PR/8 HA titer for mice immunized with PR/8 in Imiquimod-SE. **(K)** Survival of control and αv-CD19 mice following intranasal infection with PR/8 (n ≥ 5 mice/group). **(L)** Anti-PR8 HA titers from surviving mice at day 7 after infection. All data points represent individual mice with mean shown. *p*-values < 0.05 (Mann-Whitney-Wilcoxon test for antibody titers or Mantel-Cox test for survival curves) are shown and indicated by * ($p < 0.05$) or ** ($p < 0.005$). Samples below the level of detection are indicated as not detected (ND). For all data, similar results were seen in at least 3 independent experiments.

References

1. Victora GD, and Nussenzweig MC. Germinal centers. *Annu Rev Immunol.* 2012;30:429-57.
2. Bannard O, and Cyster JG. Germinal centers: programmed for affinity maturation and antibody diversification. *Curr Opin Immunol.* 2017;45:21-30.
3. DeFranco AL. The germinal center antibody response in health and disease. *F1000Res.* 2016;5.
4. Rookhuizen DC, and DeFranco AL. Toll-like receptor 9 signaling acts on multiple elements of the germinal center to enhance antibody responses. *Proc Natl Acad Sci U S A.* 2014;111(31):E3224-33.
5. Kasturi SP, Skountzou I, Albrecht RA, Koutsonanos D, Hua T, Nakaya HI, et al. Programming the magnitude and persistence of antibody responses with innate immunity. *Nature.* 2011;470(7335):543-7.
6. DeFranco AL, Rookhuizen DC, and Hou B. Contribution of Toll-like receptor signaling to germinal center antibody responses. *Immunol Rev.* 2012;247(1):64-72.
7. Leadbetter EA, Rifkin IR, Hohlbaum AM, Beaudette BC, Shlomchik MJ, and Marshak-Rothstein A. Chromatin-IgG complexes activate B cells by dual engagement of IgM and Toll-like receptors. *Nature.* 2002;416(6881):603-7.
8. Teichmann LL, Schenten D, Medzhitov R, Kashgarian M, and Shlomchik MJ. Signals via the adaptor MyD88 in B cells and DCs make distinct and synergistic contributions to immune activation and tissue damage in lupus. *Immunity.* 2013;38(3):528-40.
9. Jackson SW, Scharping NE, Kolhatkar NS, Khim S, Schwartz MA, Li QZ, et al. Opposing impact of B cell-intrinsic TLR7 and TLR9 signals on autoantibody repertoire and systemic inflammation. *J Immunol.* 2014;192(10):4525-32.
10. Acharya M, Sokolovska A, Tam JM, Conway KL, Stefani C, Raso F, et al. alphav Integrins combine with LC3 and atg5 to regulate Toll-like receptor signalling in B cells. *Nat Commun.* 2016;7:10917.
11. Barton GM, and Kagan JC. A cell biological view of Toll-like receptor function: regulation through compartmentalization. *Nat Rev Immunol.* 2009;9(8):535-42.
12. Kagan JC, Su T, Horng T, Chow A, Akira S, and Medzhitov R. TRAM couples endocytosis of Toll-like receptor 4 to the induction of interferon-beta. *Nat Immunol.* 2008;9(4):361-8.
13. Husebye H, Halaas O, Stenmark H, Tunheim G, Sandanger O, Bogen B, et al. Endocytic pathways regulate Toll-like receptor 4 signaling and link innate and adaptive immunity. *EMBO J.* 2006;25(4):683-92.
14. Sasai M, Linehan MM, and Iwasaki A. Bifurcation of Toll-like receptor 9 signaling by adaptor protein 3. *Science.* 2010;329(5998):1530-4.
15. Sanjuan MA, Dillon CP, Tait SW, Moshiach S, Dorsey F, Connell S, et al. Toll-like receptor signalling in macrophages links the autophagy pathway to phagocytosis. *Nature.* 2007;450(7173):1253-7.
16. Wang X, Rodda LB, Bannard O, and Cyster JG. Integrin-mediated interactions between B cells and follicular dendritic cells influence germinal center B cell fitness. *J Immunol.* 2014;192(10):4601-9.
17. Jegerlehner A, Maurer P, Bessa J, Hinton HJ, Kopf M, and Bachmann MF. TLR9 signaling in B cells determines class switch recombination to IgG2a. *J Immunol.* 2007;178(4):2415-20.
18. Hou B, Saudan P, Ott G, Wheeler ML, Ji M, Kuzmich L, et al. Selective utilization of Toll-like receptor and MyD88 signaling in B cells for enhancement of the antiviral germinal center response. *Immunity.* 2011;34(3):375-84.
19. Martinez J, Malireddi RK, Lu Q, Cunha LD, Pelletier S, Gingras S, et al. Molecular characterization of LC3-associated phagocytosis reveals distinct roles for Rubicon, NOX2 and autophagy proteins. *Nat Cell Biol.* 2015;17(7):893-906.

20. Tiller T, Busse CE, and Wardemann H. Cloning and expression of murine Ig genes from single B cells. *J Immunol Methods.* 2009;350(1-2):183-93.
21. Pappas L, Foglierini M, Piccoli L, Kallewaard NL, Turrini F, Silacci C, et al. Rapid development of broadly influenza neutralizing antibodies through redundant mutations. *Nature.* 2014;516(7531):418-22.
22. Clegg CH, Roque R, Van Hoeven N, Perrone L, Baldwin SL, Rininger JA, et al. Adjuvant solution for pandemic influenza vaccine production. *Proc Natl Acad Sci U S A.* 2012;109(43):17585-90.
23. Goff PH, Hayashi T, Martinez-Gil L, Corr M, Crain B, Yao S, et al. Synthetic Toll-like receptor 4 (TLR4) and TLR7 ligands as influenza virus vaccine adjuvants induce rapid, sustained, and broadly protective responses. *J Virol.* 2015;89(6):3221-35.
24. Van Hoeven N, Fox CB, Granger B, Evers T, Joshi SW, Nana GI, et al. A Formulated TLR7/8 Agonist is a Flexible, Highly Potent and Effective Adjuvant for Pandemic Influenza Vaccines. *Sci Rep.* 2017;7:46426.
25. Browne EP. Toll-like receptor 7 controls the anti-retroviral germinal center response. *PLoS Pathog.* 2011;7(10):e1002293.
26. Clingan JM, and Matloubian M. B Cell-intrinsic TLR7 signaling is required for optimal B cell responses during chronic viral infection. *J Immunol.* 2013;191(2):810-8.
27. Gianni T, Leoni V, Chesnokova LS, Hutt-Fletcher LM, and Campadelli-Fiume G. alphavbeta3-integrin is a major sensor and activator of innate immunity to herpes simplex virus-1. *Proc Natl Acad Sci U S A.* 2012;109(48):19792-7.
28. Lucas M, Stuart LM, Zhang A, Hodivala-Dilke K, Febbraio M, Silverstein R, et al. Requirements for apoptotic cell contact in regulation of macrophage responses. *J Immunol.* 2006;177(6):4047-54.
29. Savill J, Dransfield I, Hogg N, and Haslett C. Vitronectin receptor-mediated phagocytosis of cells undergoing apoptosis. *Nature.* 1990;343(6254):170-3.
30. Lacy-Hulbert A, Ueno T, Ito T, Jurewicz M, Izawa A, Smith RN, et al. Beta 3 integrins regulate lymphocyte migration and cytokine responses in heart transplant rejection. *Am J Transplant.* 2007;7(5):1080-90.
31. Overstreet MG, Gaylo A, Angermann BR, Hughson A, Hyun YM, Lambert K, et al. Inflammation-induced interstitial migration of effector CD4(+) T cells is dependent on integrin alphaV. *Nat Immunol.* 2013;14(9):949-58.
32. Acharya M, Mukhopadhyay S, Paidassi H, Jamil T, Chow C, Kissler S, et al. alphav Integrin expression by DCs is required for Th17 cell differentiation and development of experimental autoimmune encephalomyelitis in mice. *J Clin Invest.* 2010;120(12):4445-52.
33. Martinez-Martin N, Maldonado P, Gasparrini F, Frederico B, Aggarwal S, Gaya M, et al. A switch from canonical to noncanonical autophagy shapes B cell responses. *Science.* 2017;355(6325):641-7.
34. Chen M, Hong MJ, Sun H, Wang L, Shi X, Gilbert BE, et al. Essential role for autophagy in the maintenance of immunological memory against influenza infection. *Nat Med.* 2014;20(5):503-10.
35. Pengo N, Scolari M, Oliva L, Milan E, Mainoldi F, Raimondi A, et al. Plasma cells require autophagy for sustainable immunoglobulin production. *Nat Immunol.* 2013;14(3):298-305.
36. Ahmed R, and Gray D. Immunological memory and protective immunity: understanding their relation. *Science.* 1996;272(5258):54-60.
37. Pulendran B, and Ahmed R. Translating innate immunity into immunological memory: implications for vaccine development. *Cell.* 2006;124(4):849-63.
38. Querec T, Bennouna S, Alkan S, Laouar Y, Gorden K, Flavell R, et al. Yellow fever vaccine YF-17D activates multiple dendritic cell subsets via TLR2, 7, 8, and 9 to stimulate polyvalent immunity. *J Exp Med.* 2006;203(2):413-24.
39. Reed SG, Orr MT, and Fox CB. Key roles of adjuvants in modern vaccines. *Nat Med.* 2013;19(12):1597-608.

40. Desgrosellier JS, and Cheresh DA. Integrins in cancer: biological implications and therapeutic opportunities. *Nat Rev Cancer.* 2010;10(1):9-22.
41. Byron A, Humphries JD, Askari JA, Craig SE, Mould AP, and Humphries MJ. Anti-integrin monoclonal antibodies. *J Cell Sci.* 2009;122(Pt 22):4009-11.
42. Zhang Z, Goldschmidt T, and Salter H. Possible allelic structure of IgG2a and IgG2c in mice. *Mol Immunol.* 2012;50(3):169-71.
43. Schwartz MA, Kolhatkar NS, Thouvenel C, Khim S, and Rawlings DJ. CD4+ T cells and CD40 participate in selection and homeostasis of peripheral B cells. *J Immunol.* 2014;193(7):3492-502.